Translational Oncology 14 (2021) 100997

Contents lists available at ScienceDirect

Translational Oncology

journal homepage: www.elsevier.com/locate/tranon

Original Research

Mutant myogenin promoter-controlled oncolytic adenovirus selectively kills PAX3-FOXO1-positive rhabdomyosarcoma cells ☆

Hideki Yoshida [a], Mizuho Sato-Dahlman [a,b], Praveensingh Hajeri [a], Kari Jacobsen [a], Lisa Koodie [a], Chikako Yanagiba [a], Ryan Shanley [c], Masato Yamamoto [a,b,d,*]

[a] Department of Surgery, University of Minnesota, Moos Tower 11-216, MMC195, 515 Delaware St SE, Minneapolis, MN 55455, United States
[b] Masonic Cancer Center, University of Minnesota, Minneapolis, MN 55455, United States
[c] Masonic Cancer Center, Biostatistics Core, University of Minnesota, Minneapolis, MN 55455, United States
[d] Stem Cell Institute, University of Minnesota, Minneapolis, MN 55455, United States

ARTICLE INFO

Keywords:
Child cancer
Fusion-gene
MEF2
Soft-tissue sarcoma
Virotherapy

ABSTRACT

The PAX3-FOXO1 fusion gene functions as a transactivator and increases expression of many cancer-related genes. These lead to metastases and other unfavorable outcomes for alveolar rhabdomyosarcoma (ARMS) patients. In order to target ARMS with the PAX3-FOXO1 transactivator, we developed an Oncolytic Adenovirus (OAd) regulated by the myogenin (pMYOG) promoter with a mutation in the Myocyte Enhancer Factor-2 binding site (mMEF2) in this study. The expression of MYOG in the two RMS cell lines (Rh30; PAX3-FOXO1-positive, RD; PAX3-FOXO1-negative) is about 1,000 times higher than normal skeletal muscle cell (SkMC). Ad5/3-pMYOG(*S*)-mMEF2 (short-length pMYOG-controlled OAd with mMEF2) showed strong replication and cytocidal effect in Rh30, but to a much lesser extent in RD. Ad5/3-pMYOG(S) (pMYOG-controlled OAd with native pMYOG) showed similar effects in RD and Rh30. Neither virus killed SkMC, indicating that Ad5/3-pMYOG(*S*)-mMEF2 selectively replicates and kills cells with PAX3-FOXO1. Additionally, Ad5/3-pMYOG(*S*)-mMEF2 showed replication and spread *in vitro* as well as tumor growth suppression and intratumoral viral spread *in vivo*, selectively in Rh30 not in RD. Our findings revealed that Ad5/3-pMYOG(*S*)-mMEF2 shows a promise as a safe and potent therapy to improve treatment in PAX3-FOXO1-positive ARMSs.

Introduction

Rhabdomyosarcoma (RMS) is a malignant skeletal muscle tumor that occurs mainly in children and adolescents [1]. Multimodal therapy has achieved about a 60% 5-year overall survival rate of patients diagnosed with RMS. However, cure rates have not improved much since the 1990s [2,3]. RMSs are categorized into two main subtypes: alveolar RMS (ARMS) and embryonal RMS (ERMS), each containing distinct genetic abnormalities [4]. 60–70% of patients with ARMS harbor an abnormal fusion gene, *PAX3 -FOXO1*, which significantly contributes to RMS oncogenesis [5-8]. In 2010, Williamson et al. revealed that the prognosis of PAX3-FOXO1-positive ARMS is worse than that of PAX3-FOXO1-negative ARMS or ERMS with a median 5-year overall survival rate of 70% *vs* 20%, respectively [9]. This suggests that PAX3-FOXO1 is a more critical factor in risk stratification of RMS than histology. Development of novel therapeutics targeting PAX3-FOXO1 transactivator therefore has a possibility to improve clinical outcomes of RMSs.

Virotherapy has been a recent focus for as a promising approach for cancer treatment. [10-12]. In particular, adenovirus is attractive for virotherapy because 1) they can infect various cells efficiently *in vivo*, 2) they can carry large transgenes, and 3) they are not integrated into the genome, meaning lower risk of insertion mutagenesis. Adenovirus serotype 5 (Ad5), which belongs to subgroup C, is the most extensively used in virotherapy [13]. Oncolytic adenoviruses (OAds) selectively replicate in the cancer cells and kills them, subsequently causing anatomical distraction and immune-stimulation in the tumor locale [14]. One way to generate cancer specificity of OAds is controlling the expression of the adenovirus E1-gene by promoters only active in the target tumors [15-18].

Myogenic regulatory factor family (MRF) members play important roles for the process of skeletal muscle differentiation [19,20]. One

Abbreviations: Ad5, adenovirus serotype 5; ARMS, alveolar rhabdomyosarcoma; mMEF2, mutation in Myocyte Enhancer Factor-2 binding site; MRF, Myogenic regulatory factor family; MYOD, myogenic differentiation-1; pMYOG, myogenin promoter; OAd, oncolytic adenovirus; 5/3F, 5/3 fiber (a chimeric fiber containing the Ad5 shaft and Ad3 knob).

☆ Financial support: Partly supported by the Karen Wyckoff Rein in Sarcoma Foundation, and NIH/NCI: R01CA228760, R01CA196215, R01CA168448

* Corresponding author.
E-mail address: yamam016@umn.edu (M. Yamamoto).

https://doi.org/10.1016/j.tranon.2020.100997
Received 25 November 2020; Accepted 9 December 2020

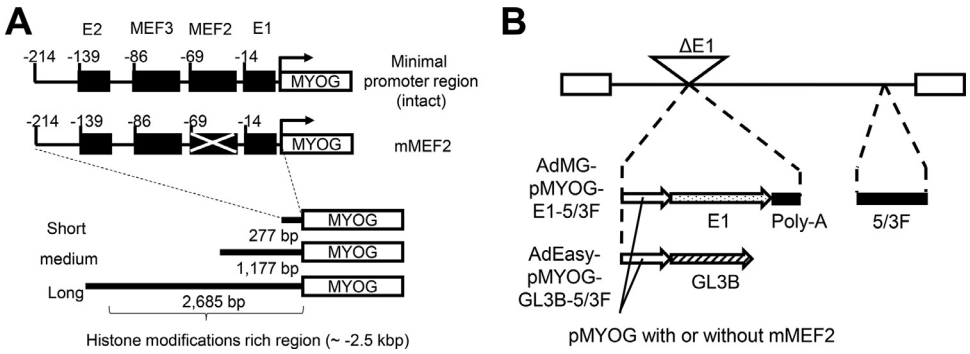

Fig. 1. Map of myogenin promoter (pMYOG) region in human and pMYOG-controlled adenovirus
A, (Top) Schematic illustration of natural and mutated −214 bp minimal pMYOG region. Arrows indicate transcription initiation site of myogenin. E1, E (enhancer)-box 1; E2, E-box 2; MEF2, myocyte enhancer factor-2 binding site; MEF3, myocyte enhancer factor-3 binding site. (Bottom) Three lengths of pMYOG used in this study. The sequence of Short contains the −214 bp minimal pMYOG region.
B, Structure of pMYOG-controlled adenovirus. The vectors were constructed based on human adenovirus type 5. pMYOG-driven E1-gene or GL3B luciferase expression cassette was inserted in the corresponding position. The E3 region of AdEasy-pMYOG-GL3B-5/3F (non-replicative) was removed, while that of Ad5/3-pMYOG (replicative) was maintained. pMYOG, myogenin promoter; mMEF2, mutation of MEF2 binding site; E1, adenovirus E1-gene 1; GL3B, luciferase reporter gene.

member of MRF, myogenin (MYOG), which acts downstream of myogenic differentiation-1 (MYOD), activates the myogenic differentiation program along with other MRFs [21-23]. Zhang et al. showed that in addition to MYOD,PAX3-FOXO1 is also an upstream regulator of MYOG via interaction with promoter of MYOG [24]. Myocyte enhancer factor-2 (MEF2) is a transcription factor that regulates cellular differentiation and embryonic development [25]. When the MEF2 binding site in the MYOG promoter (pMYOG) was mutated (mMEF2) (Fig. 1A), transactivation by MYOD was significantly reduced, but transactivation by PAX3-FOXO1 was not affected [24]. This means that pMYOG with mMEF2 can be activated in PAX3-FOXO1-positive RMS but not in PAX3-FOXO1-negative RMS or normal muscles.

Therefore, we hypothesized that pMYOG-controlled OAds can attack RMS cells with high expression of MYOG, and the OAd with mMEF2 (Ad5/3-pMYOG-mMEF2) selectively replicates and kills PAX3-FOXO1-positive RMS. In this study, we made a series of pMYOG-controlled OAds and compared their replication and cytocidal effects against multiple control viruses *in vitro* and *in vivo*. We demonstrate that OAd controlled by pMYOG with MEF2 mutation could be a powerful therapeutic approach to treating PAX3-FOXO1-positive refractory RMSs.

Materials and methods

Cell lines

Two human RMS cell lines (Rh30; PAX3-FOXO1-positive, RD; PAX3-FOXO1-negative) and HEK293 were purchased from ATCC (#CRL-2061, #CCL-136, and #CRL-1573). Another human RMS cell line, JR1 (PAX3-FOXO1-negative), was kindly provided by Dr. Subramanian (University of Minnesota, MN, USA). Human normal skeletal muscle cell (SkMC) was purchased from Lonza (#CC-2561). All RMS cell lines were maintained in RPMI-1640 (Corning). HEK293 cell line was maintained in DMEM (Corning). Both of the mediums were supplemented with 10% fetal bovine serum (FBS), 100 U/ml penicillin and 10 mg/ml streptomycin (Corning). SkMC was maintained in Skeletal muscle basal medium (SkBM-2, Lonza) supplemented with hEGF, Dexamethasone, L-glutamine, and gentamicin (Lonza), as well as 10% FBS as described in the manufacturer's instruction. All cells were cultured at 37 °C and 5% CO2. All cell lines were routinely PCR-tested for Mycoplasma. All experiments were performed using cells that have gone through less than 35 passages.

Generation of PAX3-FOXO1- and MYOD-overexpression HEK293 cells

Human *PAX3-FOXO1* and *MYOD* cDNA was cloned from Rh30 and RD, respectively, and re-cloned into pcDNA3.1(+) expression vector (Invitrogen) using *Bam*HI and *NotI* sites. HEK293 cells were plated in a 60-mm plastic plate and then transfected with the plasmids by using Superfect (Qiagen). Stable transfectants were isolated in the presence of 600 μg/ml G418 (Roche). Primers are listed in Supplement Table S1.

Generation of mutated MEF2 binding site in pMYOG

The MEF2 binding site in pMYOG was mutated with QuikChange Site-Directed Mutagenesis Kit (Agilent Technologies, Santa Clara) by inverse PCR according to the manufacturer's instructions, using the each length of pMYOG (pMYOG(S), (M), and(L)) as a template (Fig. 1A). Mutations of interest were confirmed via Sanger sequencing (Supplementary Fig. S2). The primers are described in Supplementary Table S1.

Designing plasmid including pMYOG and production of adenovirus

Reporter-expressing replication-deficient Ads and oncolytic Ads were generated as follows (Fig. 1B). Three lengths of pMYOG were cloned from the Rh30 gene within the genome. After confirming the sequences, six kinds of pMYOG (Fig. 1A), pShuttle-GL3B (8533 bp; Supplementary Fig. S1A, [26]), and pGL3-Basic (4818 bp; Promega; #E1751) were digested with *KpnI* and *NheI*. Digestion products were ligated using the Fast-Link DNA Ligation Kit (epicentre) according to the manufacturer's instructions.

While making pShuttle-pMYOG-E1, four kinds of pMYOG (Long and Short, and with or without mMEF2) and E1-gene plus protein IX (pIX) region (total 3235 bp) were amplified via PCR using Phusion High-Fidelity DNA polymerase (New England BioLabs) according to the manufacturer's instructions. In parallel, the sequence between the two *SalI* sites (nucleotides 750 and 5497) of the backbone from pShuttle-Cox2LH-E1-XpIXF (11,692 bp; Supplementary Fig. S1B, [18]) was amplified. The insert PCR products (pMYOG, E1, and pIX) were inserted into the linear plasmid backbone using the In-Fusion HD Coning Kit (Takara Bio USA) according to the manufacturer's instructions.

The ligation or in-fusion products were transformed into competent cells to amplify. The resulting plasmids of interest were extracted by Plasmid Plus Maxi Kit (Qiagen). The plasmids were linearized with *PmeI* and subsequently co-transformed into *E. coli* BJ5183 cells (Agilent Technologies) with an adenoviral backbone plasmid that is either replication

deficient (pAdEasy-5/3F) or replication competent (pMG553). All adenovirus backbones were based on human adenovirus type 5. Finally, the linearized recombinant plasmids were transfected into HEK293. Recombinant adenoviruses were generated around 10 days. The primers are listed in Supplement Table S1.

Luciferase reporter assay by plasmid transfection or virus infection

Cells (5×10^4) were plated in 24-well plates and transfected with pShuttle-pMYOG-GL3B and pGL3-basic respectively using Superfect (Qiagen) according to the manufacturer's instructions. The same cultures cells were infected with AdEasy-pMYOG-GL3B-5/3F at 10 vp/cell. Two days after transfection or infection, luciferase activity was determined with a Luciferase Assay System (Promega).

Real-time RT-PCR

Total RNA was extracted using RNeasy mini kit (Qiagen), and cDNA was synthesized with the SuperScript VILO cDNA Synthesis Kit (Thermo Fisher Scientific) according to the manufacturer's instructions, respectively. The primers are listed in Supplement Table S1. Real-time RT-PCR was carried out using the LightCycler 480 System (Roche) with SYBR Green (Applied Biosystems). Relative target mRNA expression was normalized to GAPDH using the $\Delta\Delta C_T$ method for analysis.

Binding assay

One day after seeding (1×10^5 cells/12-well plate), cells were infected with virus at 100 vp/cell. After two hours of incubation at 4 °C to prevent internalization of the virus into the cells, cells were washed with PBS, and the DNA was isolated. The viral infectivity was shown as E4-gene copy number per ng DNA as we described previously [27].

Analysis of viral replication

Cells in 12-well plates (1×10^5 cells per well) were infected with virus (0.1 to100 vp/cell), and the growth medium was harvested at 2 and 5 days after infection to assess progeny production. To collect released viral particles, medium was transferred to fresh tubes. The cells were re-suspended in PBS, and three freeze-thaw cycles were carried out to recover the virus in the cell membrane. Both the medium and viral solution were treated with 0.1 U/μl of DNaseI at 37 °C for 1 hour to eliminate non-capsidated virus DNA. The DNA was then isolated using the QIAamp DNA Mini Kit (Qiagen). The total viral copy number of the E4-gene was analyzed by qPCR using SYBR Green as described in **Real time RT-PCR section**.

In vitro *analysis of cytocidal effect by crystal violet staining*

A total of 1×10^5 cells was plated in 12-well plates and infected with virus at 0.1 to 1000 vp/cell in 1 ml of growth medium with 5% FBS. When Ad5/3-pMYOG(S) killed the cells with 10 vp/cell (low titer) or 100 vp/cell (high titer), plates were fixed with 10% buffered formalin for 10 min, stained with 1% crystal violet in 70% ethanol for 20 min, washed with water, and dried. In SkMC, both pMYOG-controlled OAds did not kill any cells, so they were fixed and stained 10 (high titer) or 14 days (low titer) after infection.

In vivo *experiment*

All animal studies were approved by the Institutional Animal Care Use Committee (IACUC) of University of Minnesota. To analyze the antitumor effect in an *in vivo* model, 2×10^6 of Rh30 or RD cells were inoculated subcutaneously into the flank of 24 nude mice (Charles River Laboratories) or 12 NSG mice (Jackson Laboratories), respectively. The same number of male and female mice were used in the experiment. 3×10^{10} vp of virus was intratumorally injected when the diameter reached 5–7 mm. The condition of the mice was monitored daily, and the tumor diameter was measured twice a week. The tumor volume was calculated as width$^2\times$length/2.

In a separate experiment under the same conditions, the mice were sacrificed at day 5 and 10. Half of each tumor specimen was quickly frozen, and the second half was fixed with buffered 4% formaldehyde for immunostaining. The DNA was purified from frozen tumor tissue using the DNeasy Blood & Tissue Kit (Qiagen) according to the manufacturer's instructions, and the adenoviral DNA copy number of the E4-gene was quantified by qPCR using SYBR Green. The expression of hexon protein in the tumor was analyzed by immunostaining using the FITC-labeled anti-hexon polyclonal antibody (Millipore; #AB1056F) and counterstained with DAPI (Vector Laboratories; #H-1200) as described in ref [18,28]. The tissues were observed with the automated upright microscope System DM5500B (Leica Biosystems).

Statistical analysis

Statistical comparisons between two groups were evaluated by Student's *t*-test. Continuous variables were compared by Mann–Whitney U test. All p-values were two-sided, and $p < 0.05$ was considered statistically significant.

As a trend analysis, the data was fit to a linear mixed model (SAS proc mixed). The outcome variable was log absolute tumor volume. Predictor variables were treatment group, time (continuous), and their interaction. Random effects for each tumor were included to account for correlation among repeated measurements. The primary hypothesis tested whether the time trend differed among groups.

Results

MYOG RNA expression and binding of 5/3 fiber (5/3F) in RMS cell lines

To assess the MYOG expression level, we measured MYOG mRNA level of two RMS cell lines (Rh30 and RD) and SkMC using real-time RT-PCR (Fig. 2A). RMS cell lines had approximately 1000-times higher MYOG expression than SkMC.

Next, to optimize the adenovirus fiber for RMS cell transduction, we compared three adenovirus fibers: 1) Wild-Type –binds to Coxsackie-Adenovirus Receptor (CAR), 2) RGD – motif containing Arginine (R), Glycine (G), and Asparate (D) which binds cellular integrins $\alpha V\beta 3$ and $\alpha V\beta 5$, 3) 5/3F – a chimeric fiber containing the Ad5 shaft and Ad3 knob that binds to CD46 and desmoglein-2, which are expressed on a wide variety of human cells and tissues. Among the three fibers, 5/3F showed the highest affinity for both RMS cells and SkMC (Fig. 2B). Based on this result, we made pMYOG-controlled adenovirus with 5/3F.

The short-length pMYOG showed the best profile in RMS cells

To find the optimal length of pMYOG to control oncolytic adenovirus replication, we first compared their promoter activities in the two RMS cells with luciferase-expressing adenoviral shuttle plasmid pShuttle-pMYOG-GL3B. pMYOG(S) showed the highest promoter activity in Rh30, while pMYOG(L) exhibited the highest promoter activity in RD (Supplementary Fig. S3). To confirm the trend with more stable transfection conditions, we compared the pMYOG activities with PAX3-FOXO1 and MYOD overexpressing HEK293 cells with better transfection efficiency. Luciferase assays for these cells using pShttle-pMYOG-GL3B confirmed the same trend as observed in RMS cells. The data indicate that pMYOG(S) was strongest among the three different lengths of pMYOG (Fig. 3A).

We also tested the difference between pMYOG(S) with or without mMEF2 with less influence of surrounding vector sequences by using pGL3-BASIC plasmid in PAX3-FOXO1 and MYOD expressing HEK293 cells to assess. The activities of the promoters with and without mMEF2

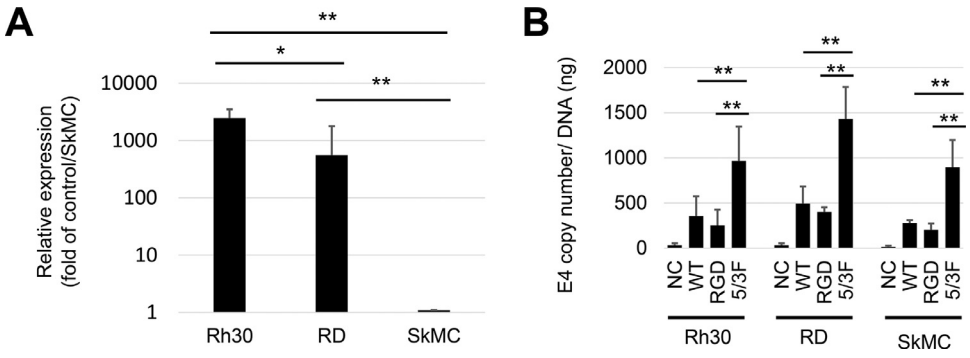

Fig. 2. Quantification of promoter activity and replication of modified virus in two rhabdomyosarcoma cells and normal muscles cell.
A, The mRNA expression of MYOG was analyzed by qPCR. After normalizing cell levels against GAPDH, the expression was shown as the relative values against that in SkMC. Results represent the means ∓ s.d. from three independent experiments. *, $P<0.05$; **, $P<0.01$.
B, Binding of the viruses with different fibers (AdEasy-GL3B-WT/ -RGD/ −5/3F). The isolated total DNA was analyzed using qPCR with primers for E4-gene to determine the adenoviral copy number bound to the surface of the cells. The number was normalized by DNA (ng). **, $P<0.01$. NC, Normal control (No infection); WT, Ad5 wild type; RGD, Integrin-binding motif; 5/3F, Chimeric fiber that contains Ad5 fiber with an Ad3 knob.

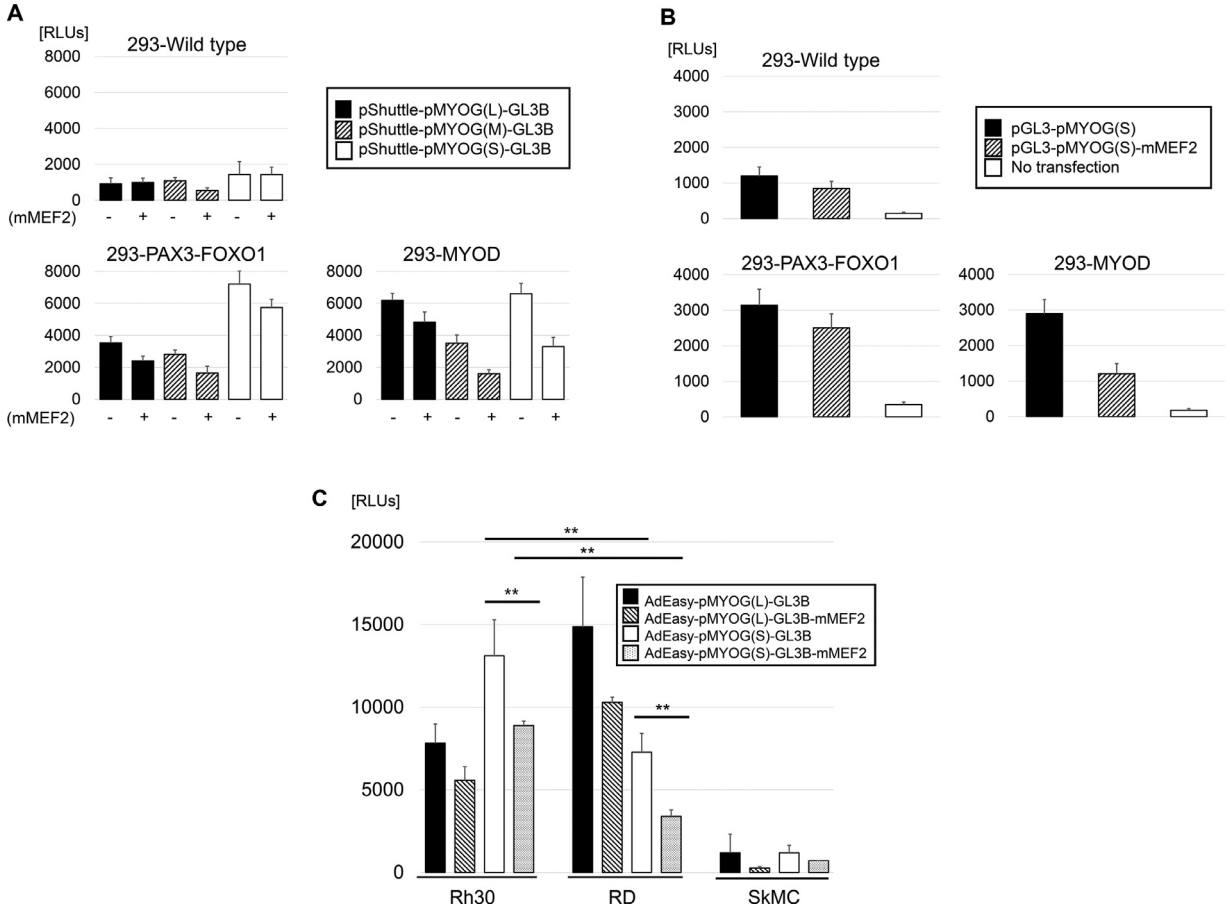

Fig. 3. Luciferase assay for HEK293 (wild-type, with PAX3-FOXO1 or MYOD) and RMS cells.
A, 1 μg pShuttle-pMYOG-GL3B were transfected into target cells. Three lengths of pMYOG (Long; 2.7 kb, Medium; 1.1 kb, Short; 0.3 kb), each with or without mMEF2, were tested to determine which length showed the greatest promoter activity. Results represent the means ∓ s.d. from three independent experiments. **B,** 1 μg pGL3B-pMYOG were transfected to the target cells. pMYOG(S) with or without mMEF2 was used to assess the influence of PAX3-FOXO1 and MYOD on the mutation in the MEF2 binding site. Results represent the means ∓ s.d. from three independent experiments. **c,** Luciferase assays of RMS cell lines infected with pMYOG-controlled adenoviruses. The infectivity enhancement was analyzed using long- and short-length pMYOG-driven luciferase expression vectors with and without mMEF2. Results represent the means ∓ s.d. from three independent experiments. **, $P<0.01$.

were smaller in HEK293-PAX3-FOXO1, while the activity of pGL3-pMYOG(*S*)-mMEF2 was lower in HEK293-MYOD (Fig. 3B). The mutation in MEF2 (mMEF2) reduced the transactivation by MYOD, but not the transactivation by PAX3-FOXO1.

Next, we compared the viruses with short- and long-length pMYOG placed in the adenovirus genome (AdEasy-pMYOG(*S*)−5/3F and AdEasy-pMYOG(L)−5/3F) with or without mMEF2 in RMS cells and SkMC. AdEasy-pMYOG(*S*)−5/3F showed high expression of luciferase in Rh30 cells but low expression in RD cells (Fig. 3C). AdEasy-pMYOG(L)−5/3F had higher expression in RD than Rh30, suggesting that MYOD or other transactivators bound somewhere in the long promoter sequence and affected the promoter activity. However, neither of

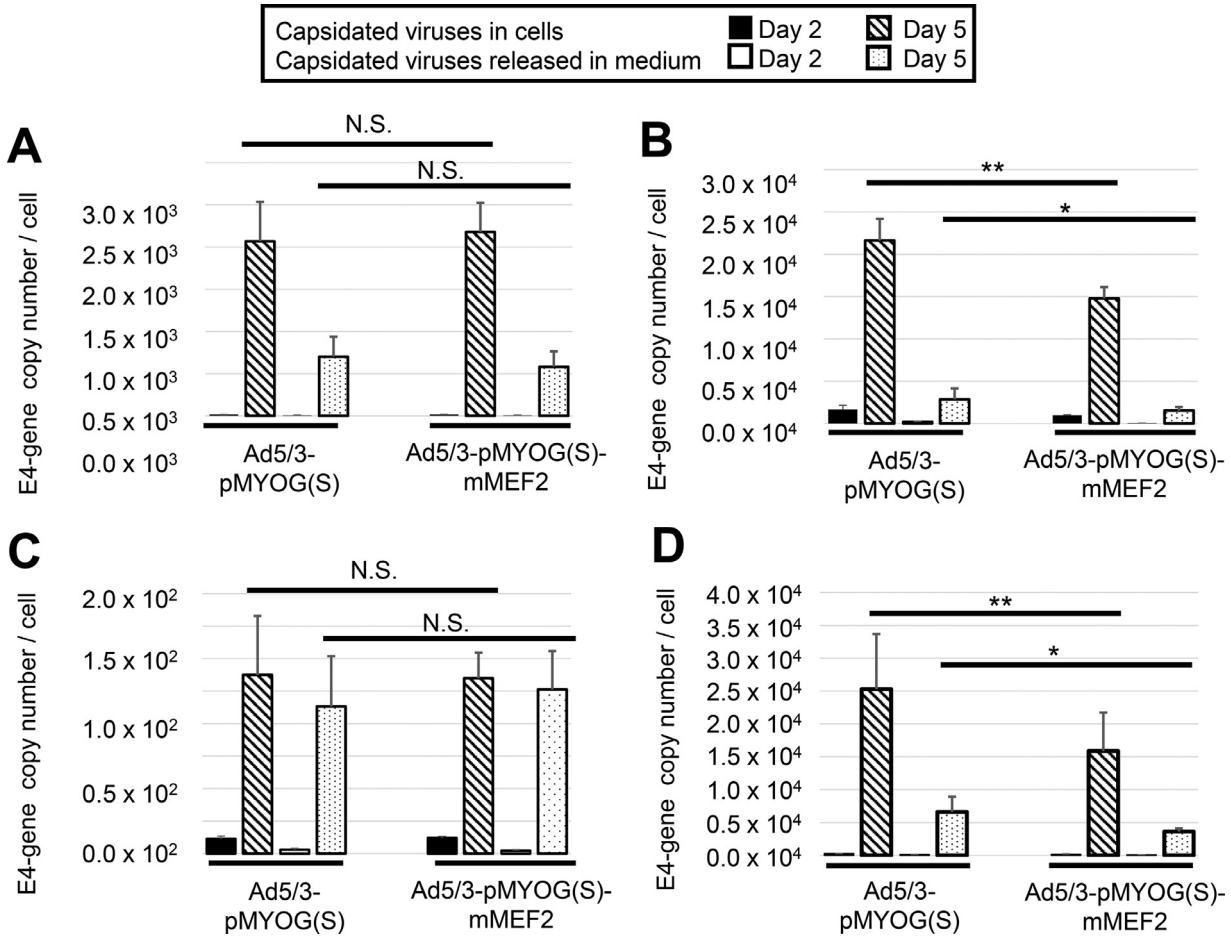

Fig. 4. Measurement of the replicating ability of pMYOG-controlled OAd *in vitro*.
Selective replication of Ad5/3-pMYOG(*S*) and Ad5/3-pMYOG(*S*)-mMEF2 in **A,** Rh30, **B,** RD, **C,** SkMC, and **D**, JR1. All three cell lines were infected with 10 vp/cell of adenovirus, and viral copy number was measured by qPCR at days 2 and 5. Results are shown as E4-gene copy number per ng DNA. Results represent the means ∓ s.d. from three independent experiments. *, $P<0.05$; **, $P<0.01$. N.S., Not Significant.

them showed promoter activity in SkMC. Therefore, we decided to use pMYOG(S) with or without mMEF2 for the following experiment.

Efficient replication and killing of pMYOG-controlled OAd with mMEF2 in PAX3-FOXO1-positive RMS cells

We next compared viral replication and cytolytic activity of pMYOG-controlled OAd in RMS cells with and without PAX3-FOXO1. Both Ad5/3-pMYOG(*S*)-mMEF2 and Ad5/3-pMYOG(S) replicated in Rh30 (Fig. 4A). In PAX3-FOX01-negative cells (RD and JR1), replication of Ad5/3-pMYOG(S) was significantly higher than Ad5/3-pMYOG(*S*)-mMEF2 (Fig. 4B and 4D). Neither of MYOGp-controlled OAds exhibited any meaningful replication in SkMC (Fig. 4C)

In the context of cytocidal effect, both pMYOG-controlled OAds with or without mMEF2 killed Rh30 under low multiplicity of infection (10 vp/cell, Fig. 5, and Supplementary Fig. S4). In RD and JR1, one order of magnitude higher amount of virus was needed for Ad5/3-pMYOG(*S*)-mMEF2 compared to Ad5/3-pMYOG(*S*). Neither of the pMYOG-controlled OAds killed SkMC with treatment as high as 1000 vp/cell, while Ad5/3 showed cytolysis at 10 vp/cell.

Tumor growth suppression and intratumoral spread of pMYOG-controlled OAd in Rh30 xenograft models

To assess the anti-tumor effect *in vivo*, pMYOG-controlled OAds were injected intratumorally into xenografts of Rh30. The administration of Ad5/3-pMYOG(S) with or without mMEF2 exhibited significant anti-tumor effect, compared to negative control (PBS) (Fig. 6A). Statistical trend analysis revealed that treatment with Ad5/3-pMYOG(*S*)-mMEF2 resulted in significantly better anti-tumor effect than Ad5/3-pMYOG(S), while the anti-tumor effect of Ad5/3-pMYOG(S) without mMEF2 mutation was significantly weaker than Ad5/3. To investigate replication and intratumoral spread of the virus, the tumor samples at day 5 and 10 in separate experiments with the same condition were assessed for viral copy number and viral structural protein (hexon) staining. The virus copy number on day 5 and 10 in tumors treated with both pMYOG-controlled OAds was like the copy number in tumors treated with Ad5/3 (Fig. 6B). There was no significant copy number increase between day 5 and day 10. The staining of virus structural protein, hexon, in the tumor specimens at days 5 and 10 after injection showed the vast majority of cells in the Rh30 tumors treated with both pMYOG-controlled OAds expressed high levels of hexon protein, which was similar to the samples treated with non-selective virus (Ad5/3) (Fig. 6C and Supplementary Fig. S5). The hexon-positive area amplified in a time-dependent manner. There was no significant difference in virus spread between pMYOG-controlled OAds with or without mMEF2 by qPCR and immunostaining.

In parallel, viral replication was assessed in PAX3-FOXO1-negative tumor (RD). The administration of Ad5/3-pMYOG(S) without mMEF2 exhibited significant antitumor effect compared to Ad5/3-pMYOG(S) with mMEF2 (Supplementary Fig. S6A). Additionally, at Day 5, the viral copy number in Ad5/3-pMYOG(S) showed a significantly higher copy number compared to Ad5/3-pMYOG(*S*)-mMEF2 (Supplementary

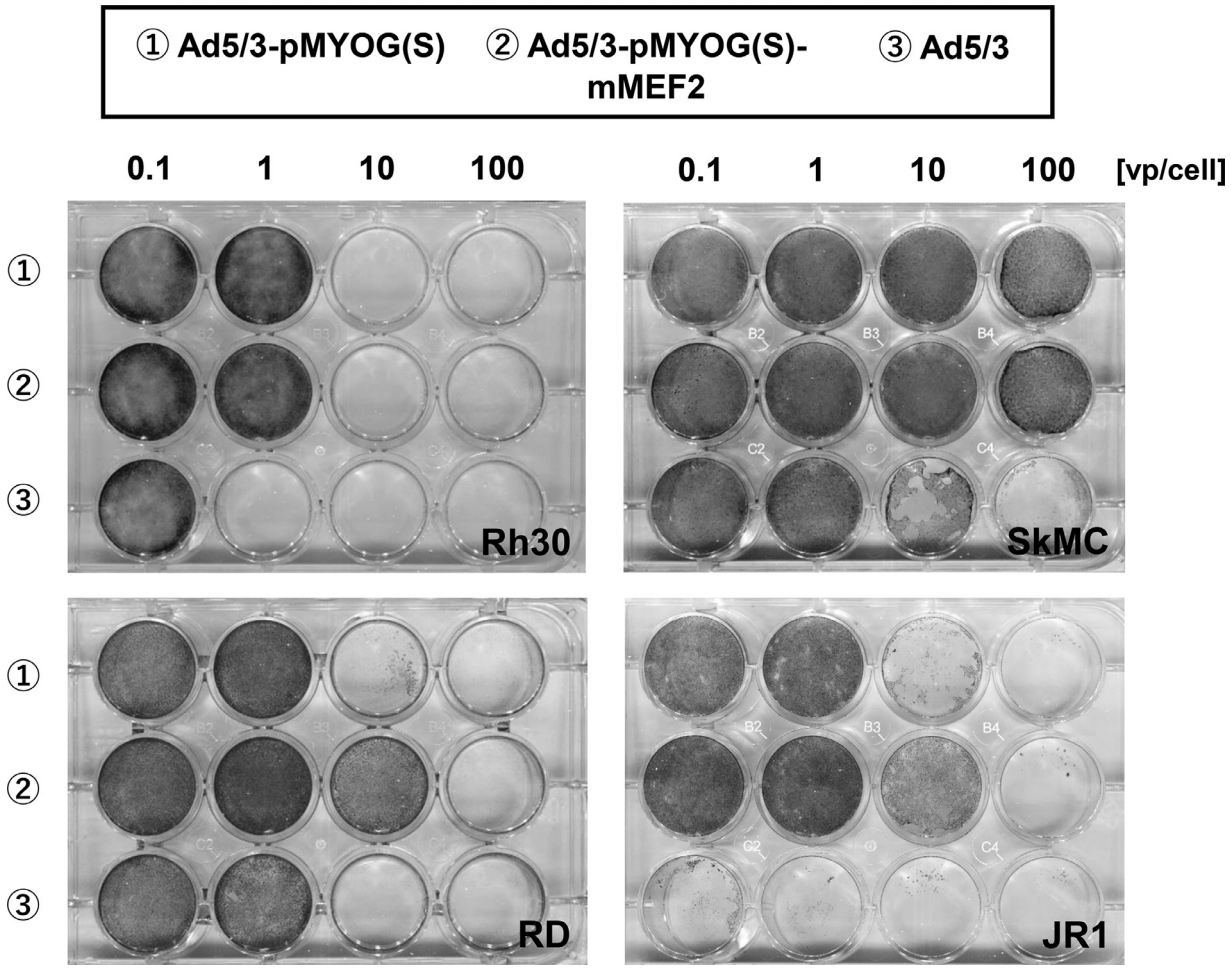

Fig. 5. Cytolytic effect of pMYOG-controlled OAd *in vitro* in low titer condition.
Cytolytic effect of Ad5/3-pMYOG(S), Ad5/3-pMYOG(*S*)-mMEF2, and Ad5/3 (with normal promoter; positive control) *in vitro*. All four cells (Rh30, RD, SkMC, and JR1) were infected with 0.1 to 100 vp/cell with the pMYOG-controlled OAd, and surviving cells were stained by crystal violet.

Fig. S6B). Furthermore, immunofluorescence staining showed stronger hexon expression in specimens injected with Ad5/3-pMYOG(S) compared those received Ad5/3-pMYOG(*S*)-mMEF2, corresponding to viral copy number analysis (Supplementary Fig. S6C).

Discussion

To develop tumor-specific promoter-controlled OAds to treat RMSs, it is essential that the controlling promoter is potent and specific to the target. Since the expression of MYOG is heavily restricted to skeletal muscle, it has been used in the diagnosis of RMS as a specific marker in combination with MYOD and Desmin [29,30]. While both ARMS and ERMS express MYOG, MYOG expression from ARMS is particularly high [29]. Our real-time RT-PCR results for both RMS cell lines and SkMC (Fig. 2A) revealed the potential to use MYOG as a target to design a novel therapy for ARMS and also indicated that pMYOG was substantially downregulated in differentiated myocytes, which corresponds with other reports [20,31]. In fact, pMYOG-controlled OAds do not replicate in SkMC (Fig. 4C) or kill them even at high titer (Fig. 5). These findings suggested that the adverse effect on normal skeletal muscle therefore will be extremely low.

We must also consider the reduction of the off-target effect on satellite cells in pMYOG-controlled OAds [24]. MYOG expresses in some organ, such as thyroid gland, mammary gland, ovary, and testis, however, its expression is much lower than that of skeletal muscle (Gene Cards, The human gene database. https://www.genecards.org/cgi-bin/carddisp.pl?gene=MYOG). Here, we evaluated the specificity of our OAd for RMS compared to normal skeletal muscle. Indeed, there is no significant difference in replication and cytolytic ability for PAX3-FOXO1-positive Rh30 between pMYOG-controlled OAds with or without mMEF2. However, the replication of OAds controlled by pMYOG with mMEF2 was 10 times lower in PAX3-FOXO1-negative RD and JR1 cells compared to OAds without MEF2 (Fig. 5 and Supplementary Figure S4). Taken together, we consider that addition of mMEF2 to pMYOG-controlled OAd increases safety by reducing toxicity in PAX3-FOXO1-negative cells, including muscle satellite cells, without compromising efficacy for PAX3-FOXO1-positive ARMS.

Faralli et al. indicated a possibility that the *Myogenin* gene has three distal enhancers (−4.5 kb, −5.5 kb, and −6.5 kb) [31], but this sequence is too long to insert into the adenovirus genome as a controlling promoter [32]. We compared three different lengths of pMYOG: 2.7 kb pMYOG(L), which has histone modifications rich region [33]; 1.1 kb pMYOG(M), which includes −1092 to −340 bp region known as enhancer element in mice [34]; and 0.3 kb pMYOG(S), mostly consisting of the "minimal promoter region" that can activate MYOG with only around 200 bases [34]. In addition, L. Zhang et al. has already clarified that the main contact part of the PAX3-FOXO1 protein is four bases from −119 to −122 of myogenin promoter [24]. pMYOG(S) with shortest promoter region showed the strongest activity in both PAX3-FOXO1-positive and PAX3-FOXO1-negative-MYOD-positive cells (Fig. 3A, C, and Supplementary Fig. S3) and exhibited the best contrast between the promoters with and without mMEF2 (Fig. 3B). Also, pMYOG(L)

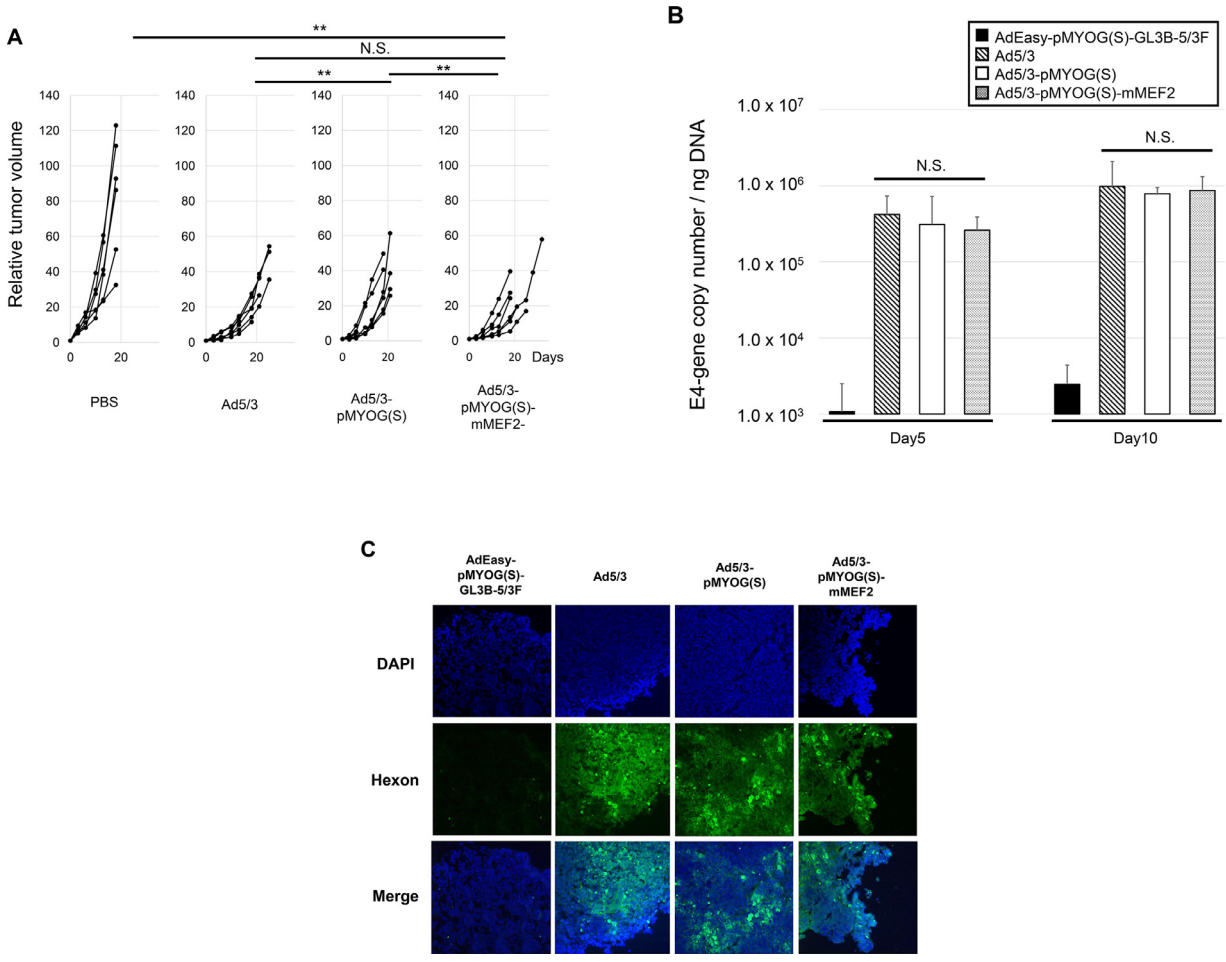

Fig. 6. Antitumor effect and virus replication of pMYOG-controlled OAd in established tumors in Rh30.
A, The anti-tumor effect of intratumorally-administered pMYOG-controlled OAd was analyzed using a Rh30 subcutaneous xenograft model. Control virus without specificity (Ad5/3), pMYOG-controlled virus (Ad5/3-pMYOG(*S*) and Ad5/3-pMYOG(*S*)-mMEF2), and PBS were injected intratumorally (3×10^{10} vp/tumor or 50μl). Each line represents relative tumor volume. $n=3$ mice per group. *, $P<0.05$; **, $P<0.01$. N.S., Not Significant. **B,** Viral copy number in tumor specimens was measured via qPCR at days 5 and 10. Results are shown as E4-gene copy number per ng DNA. *, $P<0.05$. *AdEasy-pMYOG(*S*)-GL3B, replication incompetent because of deleted E1-gene. **C,** Expression of the adenovirus late gene product hexon was assessed at day 10 by immunostaining, and nuclei were counterstained with DAPI. Green, Ad hexon protein; Blue, nucleus (magnification × 20). *AdEasy-pMYOG(*S*)-GL3B, replication incompetent because of deleted E1-gene.

showed stronger activity in PAX3-FOXO1-negative-MYOD-positive cell (Fig. 3B, C, and Supplementary Fig. S3). In this sense, pMYOG(S) is optimal for our application. The reason that pMYOG(L) showed high activity in PAX3-FOXO1-negative-MYOD-positive cells is not entirely clear, but we believe that transcription factors other than PAX3-FOXO1 and MYOD may have affected the 2.5 kb region. pMYOG(M) was not strongly activated in PAX3-FOXO1-positive or PAX3-FOXO1-negative-MYOD-positive cells, implying that there was no major enhancer element in region −1092 to −340 bp in human.

One possible way to augment the anti-tumor effect of pMYOG-controlled OAds is to change fiber to another construct that has greater affinity for RMS. Certainly, we showed 5/3F bind to RMS and SkMC the most compared with CAR and RGD, but the expression of its main targets CD46 (The human protein atlas; https://www.proteinatlas.org/ENSG00000117335-CD46/tissue, [35]) and desmoglein-2 (The human protein atlas; https://www.proteinatlas.org/ENSG00000046604-DSG2/tissue) are not particularly strong in skeletal muscle. Recently, we have reported an adenovirus library screening system that determined target-specific fiber [28,36]. If there were a se;ective RMS cell surface marker, we could modify pMYOG-controlled OAds with higher affinity and selectivity via the modified fiber. While the selectivity of OAd with mMEF2 seems sufficient for clinical development, further enhancement of specificity for ARMS can be achieved via a dual promoter-controlled system [37]. Since several genes are reported as downstream of PAX3-FOXO1, such as FGFR4, CNR1, and CCND1, these might be potential targets for future development selectivity [38,39]. Just like other virotherapies, pMYOG-controlled OAds will likely show greater potential via combination therapy with radiotherapy, cytokines, or T-cell therapy rather than using the virus alone [40-42].

Some virotherapies for RMS have been reported, including the use of adenoviruses [43-46] but has not been developed to specifically overcome PAX3-FOXO1-positive ARMS. The Children's Oncology Group (COG) performed a phase-1 trial to determine the effectiveness of virotherapy using Seneca Valley Virus for children with relapsed or refractory solid tumors, including rhabdomyosarcoma. The virotherapy was feasible and tolerable at the dose levels tested in pediatric patients [47]. These results are exciting because virotherapy has not been successful in treating childhood cancer. Neutralizing antibodies certainly lower the effectiveness when viruses are administered intravenously, including adenovirus [48]. However, there is little influence of neutralizing antibodies when adenovirus is administered intratumorally [49]. On top of that, the other oncolytic adenoviruses, such as Wnt signaling- and GOLPH2-regulated OAd, have reported recently [50,51], we believe

that this field would be an attractive option to overcome cancer in the near future.

Conclusion

OAds controlled by pMYOG with mMEF2 showed clear anti-tumor effect for RMS cell *in vitro* and *in vivo*. Our findings demonstrated that the enhanced specificity of OAd with pMYOG-mMEF2 has potential for development of therapeutics targeting PAX3-FOXO1-positive RMSs that are the most problematic type of the RMS in clinical settings. We hope our findings will become a new stepping-stone for virotherapy for childhood malignant diseases.

Funding

This research was supported by grants from Grant from Karen Wyckoff Rein in Sarcoma Foundation and NIH/NCI: R01CA228760, R01CA196215, R01CA168448 (to M. Yamamoto). The funding was used to support all study design, data analyses, and manuscript constructions.

Author's contributions

Conception and design: H.Y., M.Y. Development of methodology: H.Y., M.S.D., P.H., M.Y. Acquisition of data (provide): H.Y., C.Y. Statistics Analysis: R.S. Analysis and interpretation of data: H.Y., M.Y. Writing review, and /or revision of the manuscript: H.Y., C.Y., M.Y. Administrative, technical, or material support: M.S.D., P.H., K.J., L.K. Study supervision: M.Y.

Data and materials availability

All data generated or analyzed during this study are included in this published article and its supplementary information files.

Declaration of Competing Interest

The author declare that they have no competing interests.

Acknowledgments

We sincerely thank Dr. Subramanian for his kindness in providing JR1 cell line. Writing and editing assistance was provided by Christopher J. LaRocca, Brett Roach, and Kenta Yamamoto

Supplementary materials

Supplementary material associated with this article can be found, in the online version, at doi:10.1016/j.tranon.2020.100997.

References

[1] S. Ognjanovic, A.M. Linabery, B. Charbonneau, J.A. Ross, Trends in childhood rhabdomyosarcoma incidence and survival in the United States, 1975-2005, Cancer 115 (2009) 4218–4226, doi:10.1002/cncr.24465.
[2] I. Sultan, I. Qaddoumi, S. Yaser, C. Rodriguez-Galindo, A. Ferrari, Comparing adult and pediatric rhabdomyosarcoma in the surveillance, epidemiology and end results program, 1973 to 2005: an analysis of 2,600 patients, J. Clin. Oncol. 27 (2009) 3391–3397, doi:10.1200/jco.2008.19.7483.
[3] A.S. Pappo, D.N. Shapiro, W.M. Crist, H.M. Maurer, Biology and therapy of pediatric rhabdomyosarcoma, J. Clin. Oncol. 13 (1995) 2123–2139, doi:10.1200/jco.1995.13.8.2123.
[4] C.A. Arndt, W.M. Crist, Common musculoskeletal tumors of childhood and adolescence, N. Engl. J. Med. 341 (1999) 342–352, doi:10.1056/nejm199907293410507.
[5] P.H. Sorensen, J.C. Lynch, S.J. Qualman, R. Tirabosco, J.F. Lim, H.M. Maurer, J.A. Bridge, W.M. Crist, T.J. Triche, F.G. Barr, PAX3-FKHR and PAX7-FKHR gene fusions are prognostic indicators in alveolar rhabdomyosarcoma: a report from the children's oncology group, J. Clin. Oncol. 20 (2002) 2672–2679, doi:10.1200/jco.2002.03.137.
[6] L. del Peso, V.M. González, R. Hernández, F.G. Barr, G. Núñez, Regulation of the forkhead transcription factor FKHR, but not the PAX3-FKHR fusion protein, by the serine/threonine kinase Akt, Oncogene 18 (1999) 7328–7333, doi:10.1038/sj.onc.1203159.
[7] W.J. Fredericks, N. Galili, S. Mukhopadhyay, G. Rovera, J. Bennicelli, F.G. Barr, F.J. Rauscher 3rd, The PAX3-FKHR fusion protein created by the t (2; 13) translocation in alveolar rhabdomyosarcomas is a more potent transcriptional activator than PAX3, Mol. Cell. Biol. 15 (1995) 1522–1535, doi:10.1128/mcb.15.3.1522.
[8] J.L. Bennicelli, R.H. Edwards, F.G. Barr, Mechanism for transcriptional gain of function resulting from chromosomal translocation in alveolar rhabdomyosarcoma, Proc. Natl. Acad. Sci 93 (1996) 5455–5459, doi:10.1073/pnas.93.11.5455.
[9] D. Williamson, E. Missiaglia, A. de Reynies, G. Pierron, B. Thuille, G. Palenzuela, K. Thway, D. Orbach, M. Laé, P. Fréneaux, K. Pritchard-Jones, O. Oberlin, J. Shipley, O. Delattre, Fusion gene-negative alveolar rhabdomyosarcoma is clinically and molecularly indistinguishable from embryonal rhabdomyosarcoma, J. Clin. Oncol. 28 (2010) 2151–2158, doi:10.1200/jco.2009.26.3814.
[10] G.R. Simpson, K. Relph, K. Harrington, A. Melcher, H. Pandha, Cancer immunotherapy via combining oncolytic virotherapy with chemotherapy: recent advances, Oncolytic virother. 5 (2016) 1–13, doi:10.2147/OV.S66083.
[11] A.T. Baker, C. Aguirre-Hernández, G. Halldén, A.L. Parker, Desingner oncolytic adenovirus: coming of age, Cancers (Basel) 10 (2018) 201, doi:10.3390/cancers10060201.
[12] K. Harrington, D.J. Freeman, B. Kelly, J. Harper, J.C. Soria, Optimizing oncolytic virotherapy in cancer treatment, Nat. Rev. Drug Discov. 18 (2019) 689–706, doi:10.1038/s41573-019-0029-0.
[13] J.J. Rux, R.M. Burnett, Adenovirus structure, Hum. Gene Ther 15 (2004) 1167–1176, doi:10.1089/hum.2004.15.1167.
[14] A. Howells, G. Marelli, N.R. Lemoine, Y. Wang, Oncolytic viruses—interaction of virus and tumor cells in the battle to eliminate cancer, Front. Oncol. 7 (2017) 195, doi:10.3389/fonc.2017.00195.
[15] R. Rodriguez, E.R. Schuur, H.Y. Lim, G.A. Henderson, J.W. Simons, D.R. Henderson, Prostate attenuated replication competent adenovirus (ARCA) CN706: a selective cytotoxic for prostate-specific antigen-positive prostate cancer cells, Cancer Res. 57 (1997) 2559–2563.
[16] L. Zhang, H. Akbulut, Y. Tang, X. Peng, G. Pizzorno, E. Sapi, S. Manegold, A. Deisseroth, Adenoviral vectors with E1A regulated by tumor-specific promoters are selectively cytolytic for breast cancer and melanoma, Mol. Ther. 6 (2002) 386–393, doi:10.1006/mthe.2002.0680.
[17] J. Kim, B. Lee, J.S. Kim, C.O. Yun, J.H. Kim, Y.J. Lee, C.H. Joo, H. Lee, Antitumoral effects of recombinant adenovirus YKL-1001, conditionally replicating in α-fetoprotein-producing human liver cancer cells, Cancer Lett. 180 (2002) 23–32, doi:10.1016/s0304-3835(02)00017-4.
[18] M. Yamamoto, J. Davydova, M. Wang, G.P. Siegal, V. Krasnykh, S.M. Vickers, D.T. Curiel, Infectivity enhanced, cyclooxygenase-2 promoter-based conditionally replicative adenovirus for pancreatic cancer, Gastroenterology 125 (2003) 1203–1218, doi:10.1016/s0016-5085(03)01196-x.
[19] A.B. Lassar, R.L. Davis, W.E. Wright, T. Kadesch, C. Murre, A. Voronova, D. Baltimore, H. Weintraub, Functional activity of myogenic HLH proteins requires hetero-oligomerization with E12/E47-like proteins *in vivo*, Cell 66 (1991) 305–315, doi:10.1016/0092-8674(91)90620-e.
[20] J.M. Hernández-Hernández, E.G. García-González, M.A. Brun, C.E. Rudnicki, The myogenic regulatory factors, determinants of muscle development, cell identity and regeneration, Semin. Cell Dev. Biol. 72 (2017) 10–18, doi:10.1016/j.semcdb.2017.11.010.
[21] G. Comai, S. Tajbakhsh, Molecular and cellular regulation of skeletal myogenesis, Curr. Top. Dev. Biol. 110 (2014) 1–73, doi:10.1016/b978-0-12-405943-6.00001-4.
[22] R.L. Davis, H. Weintraub, A.B. Lassar, Expression of a single transfected cDNA converts fibroblasts to myoblasts, Cell 51 (1987) 987–1000, doi:10.1007/978-1-4684-5865-7_1.
[23] W.E. Wright, D.A. Sassoon, V.K. Lin, Myogenin, a factor regulating myogenesis, has a domain homologous to MyoD, Cell 56 (1989) 607–617, doi:10.1016/0092-8674(89)90583-7.
[24] L. Zhang, C. Wang, Identification of a new class of PAX3-FKHR target promoters: a role of the Pax3 paired box DNA binding domain, Oncogene 26 (2007) 1595–1605, doi:10.1038/sj.onc.1209958.
[25] M.J. Potthoff, E.N. Olson, MEF2: a central regulator of diverse developmental programs, Development 134 (2007) 4131–4140, doi:10.1242/dev.008367.
[26] M. Yamamoto, R. Alemany, Y. Adachi, W.E. Grizzle, D.T. Curiel, Characterization of the cyclooxygenase-2 promoter in an adenoviral vector and its application for the mitigation of toxicity in suicide gene therapy of gastrointestinal cancers, Mol. Ther. 3 (2001) 385–394, doi:10.1006/mthe.2001.0275.
[27] J. Davydova, L.P. Le, T. Gavrikova, M. Wang, V. Krasnykh, M. Yamamoto, Infectivity-enhanced cyclooxygenase-2-based conditionally replicative adenoviruses for esophageal adenocarcinoma treatment, Cancer Res 64 (2004) 4319–4327, doi:10.1158/0008-5472.can-04-0064.
[28] Y. Miura, S. Yamasaki, J. Davydova, E. Brown, K. Aoki, S. Vickers, M. Yamamto, Infectivity-selective oncolytic adenovirus developed by high-throughput screening of adenovirus-formatted library, Mol. Ther. 21 (2013) 139–148, doi:10.1038/mt.2012.205.
[29] M.H. Cessna, H. Zhou, S.L. Perkins, S.R. Tripp, L. Layfield, C. Daines, C.M. Coffin, Are myogenin and myoD1 expression specific for rhabdomyosarcoma?: A study of 150 cases, with emphasis on spindle cell mimics, Ame. J. Surg Pathol. 25 (2001) 1150–1157, doi:10.1097/00000478-200109000-00005.
[30] S. Kumar, E. Perlman, C.A. Harris, M. Raffeld, M. Tsokos, Myogenin is a specific marker for rhabdomyosarcoma: an immunohistochemical study in paraffin-embedded tissues, Mod. Pathol. 13 (2000) 988, doi:10.1038/modpathol.3880179.
[31] H. Faralli, F.J. Dilworth, Turning on myogenin in muscle: a paradigm for understanding mechanisms of tissue-specific gene expression, Comp. Funct. Genomics. 2012 (2012) 836374, doi:10.1155/2012/836374.

[32] A.J. Bett, L. Prevec, F.L. Graham, Packaging capacity and stability of human adenovirus type 5 vectors, J. Virol. 67 (1993) 5911–5921, doi:10.1128/jvi.67.10.5911-5921.1993.
[33] Z. Wang, C. Zang, J.A. Rosenfeld, D.E. Schones, A. Barski, S. Cuddapah, K. Cui, T.Y. Roh, W. Peng, M.Q. Zhang, K. Zhao, Combinatorial patterns of histone acetylations and methylations in the human genome, Nat. Genet. 40 (2008) 897, doi:10.1038/ng.154.
[34] D.G. Edmondson, T.C. Cheng, P. Cserjesi, T. Chakraborty, E.N. Olson, Analysis of the myogenin promoter reveals an indirect pathway for positive autoregulation mediated by the muscle-specific enhancer factor MEF-2, Mol. Cell. Biol. 12 (1992) 3665–3677, doi:10.1128/mcb.12.9.3665.
[35] N. Larochelle, J.R. Deol, V. Srivastava, C. Allen, H. Mizuguchi, G. Karpati, P.C. Holland, J. Nalbantoglu, Downregulation of CD46 during muscle differentiation: implications for gene transfer to human skeletal muscle using group B adenoviruses, Hum. Gene Ther 19 (2008) 133–142, doi:10.1089/hum.2007.040.
[36] M. Sato-Dahlman, Y. Miura, J.L. Huang, P. Hajeri, K. Jacobsen, J. Davydova, M. Yamamoto, CD133-targeted oncolytic adenovirus demonstrates anti-tumor effect in colorectal cancer, Oncotarget 8 (2017) 76044, doi:10.18632/oncotarget.18340.
[37] Y. Li, N. Idamakanti, T. Arroyo, S. Thorne, T. Reid, S. Nichols, M. VanRoey, G. Colbern, N. Nguyen, O. Tam, P. Working, D.C. Yu, Dual promoter–controlled oncolytic adenovirus CG5757 has strong tumor selectivity and significant antitumor efficacy in preclinical models, Clin. Cancer Res. 11 (2005) 8845–8855, doi:10.1158/1078-0432.ccr-05-1757.
[38] C. De Pitta, L. Tombolan, G. Albiero, F. Sartori, C. Romualdi, G. Jurman, M. Carli, C. Furlanello, G. Lanfranchi, A. Rosolen, Gene expression profiling identifies potential relevant genes in alveolar rhabdomyosarcoma pathogenesis and discriminates PAX3-FKHR positive and negative tumors, Int. J Cancer. 118 (2006) 2772–2781, doi:10.1002/ijc.21698.
[39] M. Lae, E.H. Ahn, G.E. Mercado, S. Chuai, M. Edgar, B.R. Pawel, A. Olshen, F.G. Barr, M. Ladanyi, Global gene expression profiling of PAX-FKHR fusion-positive alveolar and PAX-FKHR fusion-negative embryonal rhabdomyosarcomas, J. Pathol. 212 (2007) 143–151, doi:10.1002/path.2170.
[40] A.O. Salzwedel, J. Han, C.J. LaRocca, R. Shanley, M. Yamamoto, J. Davydova, Combination of interferon-expressing oncolytic adenovirus with chemotherapy and radiation is highly synergistic in hamster model of pancreatic cancer, Oncotarget 9 (2018) 18041, doi:10.18632/oncotarget.24710.
[41] N. Nishio, I. Diaconu, H. Liu, V. Cerullo, I. Caruana, V. Hoyos, L. Bouchier-Hayes, B. Savoldo, G. Dotti, Armed oncolytic virus enhances immune functions of chimeric antigen receptor–modified T cells in solid tumors, Cancer Res. 74 (2014) 5195–5205, doi:10.1158/0008-5472.can-14-0697.
[42] A.R. Shaw, C.E. Porter, N. Watanabe, K. Tanoue, A. Sikora, S. Gottschalk, M.K. Brenner, M. Suzuki, Adenovirotherapy delivering cytokine and checkpoint inhibitor augments CAR T cells against metastatic head and neck cancer, Mol. Ther. 25 (2017) 2440–2451, doi:10.1016/j.ymthe.2017.09.010.
[43] K. Tanoue, Y. Wang, M. Ikeda, K. Mitsui, R. Irie, T. Setoguchi, S. Komiya, S. Natsugoe, K. Kosai, Survivin-responsive conditionally replicating adenovirus kills rhabdomyosarcoma stem cells more efficiently than their progeny, J. Trans. Med. 12 (2014) 27, doi:10.1186/1479-5876-12-27.
[44] M.P. Phelps, H. Yang, S. Patel, M.M. Rahman, G. McFadden, E. Chen, Oncolytic virus-mediated RAS targeting in rhabdomyosarcoma, Mol. Ther. Oncol. 11 (2018) 52–61, doi:10.1016/j.omto.2018.09.001.
[45] B. Hutzen, C.Y. Chen, P.Y. Wang, L. Sprague, H.M. Swain, J. Love, J. Conner, L. Boon, T.P. Cripe, Tgf-β inhibition improves oncolytic herpes viroimmunotherapy in murine models of rhabdomyosarcoma, Mol. Ther. Oncol. 7 (2017) 17–26, doi:10.1016/j.omto.2017.09.001.
[46] C.C. Dobson, T. Naing, S.T. Beug, M.D. Faye, J. Chabot, M. St-Jean, D.E. Walker, E.C. LaCasse, D.F. Stojdl, R.G. Korneluk, M. Holcik, Oncolytic virus synergizes with Smac mimetic compounds to induce rhabdomyosarcoma cell death in a syngeneic murine model, Oncotarget 8 (2017) 3495, doi:10.18632/oncotarget.13849.
[47] M.J. Burke, C. Ahern, B.J. Weigel, J.T. Poirier, C.M. Rudin, Y. Chen, T.P. Cripe, M.B. Bernhardt, S.M. Blaney, Phase I trial of Seneca valley virus (NTX-010) in children with relapsed/refractory solid tumors: a report of the children's oncology group, Pediatr. Blood Cancer. 62 (2015) 743–750, doi:10.1002/pbc.25269.
[48] N. Chirmule, K.J. Propert, S.A. Magosin, Y. Qian, R. Qian, J.M. Wilson, Immune responses to adenovirus and adeno-associated virus in humans, Gene Ther. 6 (1999) 1574–1583, doi:10.1038/sj.gt.3300994.
[49] K. Tomita, F. Sakurai, M. Tachibana, H. Mizuguchi, Correlation between adenovirus-neutralizing antibody titer and adenovirus vector-mediated transduction efficiency following intratumoral injection, Anticancer Res 32 (2012) 1145–1152.
[50] C. Ying, B.D. Xiao, Y. Qin, B.R. Wang, X.Y. Liu, R.W. Wang, L. Fang, H. Yan, X.M. Zhou, Y.G. Wang, GOLPH2-regulated oncolytic adenovirus, GD55, exerts strong killing effect on human prostate cancer stem-like cells *in vitro* and *in vivo*, Acta Pharmacol. Sin. 39 (2018) 405–414, doi:10.1038/aps.2017.91.
[51] J. Zhang, W. Lai, Q. Li, Y. Yu, J. Jin, W. Guo, X. Zhou, X. Liu, Y. Wang, A novel oncolytic adenovirus targeting Wnt signaling effectively inhibits cancer-stem like cell growth via metastasis, apoptosis and autophagy in HCC models, Biochem. Biophys. Res. Commun. 491 (2017) 469–477, doi:10.1016/j.bbrc.2017.07.041.